International Journal of Advances in Applied Sciences (IJAAS)
Vol. 13, No. 2, June 2024, pp. 234~248
ISSN: 2252-8814, DOI: 10.11591/ijaas.v13.i2.pp234-248

Simulation and modeling for controlling stepper motor with tuned PID by GWO: comparative study

Salam Waley Shneen[1], Hashmia S. Dakheel[2], Zainab B. Abdullah[2]
[1]Energy and Renewable Energies Technology Center, University of Technology, Baghdad, Iraq
[2]Department of Electro-mechanical Engineering, University of Technology, Baghdad, Iraq

Article Info

Article history:

Received Nov 7, 2023
Revised Dec 19, 2023
Accepted Jan 31, 2024

Keywords:

Closed loop
ITAE function
Open loop
PID controller
PID-GWO
Stepper motor

ABSTRACT

The current work aims to simulate the operation of the electric motor in one of the most important industrial applications, which is printers, by adopting stepper motors (SM). The performance of the motor is also improved by adopting traditional control systems and adjusting them using the gray wolf optimization (GWO) advanced algorithm. It works to adjust the parameters of a conventional controller. Simulation to reach an appropriate design with high performance, which is obtained by adopting the integral time absolute error (ITAE) function to get rid of the error for transient cases. Transfer function was adopted to represent the engine and two methods of control were used, traditional and advanced optimization. Results demonstrated the possibility of improving performance by adopting both methods with a clear superiority of advanced optimization. Response of SM without controller for close loop shows the values of each rising time equal 130.440 ms, overshoot equal 0.505%, and undershoot equal 1.077%. Response of SM for close loop with proportional-integral-derivative controllers (PIDC) shows the parameters, performance, and robustness of PIDC also the values of overshoot=9.16%, settling time=0.406, and rise time=0.0628 s. Results were developed by using GWO-PID over the previous cases by reducing values of overshoot to zero, rise time, and settling time to 0.00145 and 0.0027 respectively.

Corresponding Author:

Salam Waley Shneen
Energy and Renewable Energies Technology Center, University of Technology
52 Industry Street, Baghdad, Iraq
Email: salam_waley73@yahoo.com

1. INTRODUCTION

Stepper motors (SM) are electromechanical devices that convert electrical impulses into mechanical movement on the shaft. SM has wide uses in industrial applications such as robotic arms, scanners, numerical control machines (CNC), printers, and 3D printers because SM features (high reliability, low cost, low power, fast dynamic, fast response, and accurate positioning [1], [2]. Traffic signs and signals are among the important means that regulate the movement of vehicles and individuals on the road. It is necessary to comply with these signs and signals to ensure a safe and trouble-free road. There are several ways to implement road signs using high technology, including the use of hands to carry the equipment of traffic signs and the use of trucks that are fixed to their chassis special equipment to implement straight road signs. The disadvantage of this technology appears when applying curly letters because the implementation requires a long time and ineffective manual work. Therefore, the need to use an automatic road printer appeared for applications when curvy characters and complex roads. SM is used as a motor to ensure the stability of the road printer driving system. Road printer drivers are SM. Therefore, the need arose to improve the control system in these motors to obtain better results. Road printer: It is a device designed to draw complex pictures of large sizes and dividing strips on the sidewalks. The use of a road printer gives a high technology in reducing complexity and increasing work efficiency, it consists of (a stepper motor, control device, drop guides, carriage, movable carriage, nozzle, and ink tank) [3], [4].

Proportional-integral-differentiating (PID) than the traditional controllers that are used to control the SM motor because of its simplicity, ease of implementation, and applicability. PID provides good performance with linear systems [5], [6]. In the current search, SM speed was controlled by adjusting the parameters of the PID controller by applying the Indexing and abstracting services depending on the accuracy of the title, extracting from it keywords useful in cross-referencing and computer searching. An improperly titled paper may never reach the audience for which it was intended, so be specific. Gray wolf optimization (GWO) algorithm, integral time absolute error (ITAE) was also used as an objective function. GWO is a bio-inspired guiding algorithm derived from the social hierarchy of gray wolves which represents their hunting demeanor. Search begins (solutions) in GWO which represents a randomly population of generated wolves, (optimization) process during the hunting, through an iterative procedure these wolves estimate the (optimal) location of the prey [7], [8].

Zhao *et al*. [9], researched the speed of SM was controlled using transfer function equations and a close loop control system through the PID neural network algorithm. The research used the matrix laboratory (MATLAB) simulation program, and the results were powerful, adaptable, and more accurate than conventional controllers. Mahmoud and Ramadhan [10] presented a simulation using the MATLAB program to obtain the best parameters sliding mode controllers (SMC) for the hybrid SM to obtain a stable situation of tracking the position of the rotor and a smooth transient when the load disturbances that the stepper motor is exposed to. Silaa *et al*. [11] discuss the use of an extended gray wolf optimizer (EGWO) algorithm to design a PID controller for a boost converter. The proposed system showed smooth dynamic response and fast convergence to optimal solutions with different loads. Aziz *et al*. [12] presented parameters of traditional PID controllers that were set using optimization techniques such as the GWO for the DC motor, obtaining good performance of motor work, accuracy, high speed, and better response. MATLAB simulation of a DC motor model to control its speed through fractional order PID controllers (FOPID). PID parameters are set using different methods, including traditional and modern ones, such as partial gray wolf optimization (PGWO), good motor performance, high precision, high speed and better response than traditional methods were obtained, the corresponding rising time, settling time, and maximum overshoot. This paper presents a study of using PID-GWO optimization to control SM which is used in road printers and compares these results with conventional PID controllers to improve SM performance [13].

In the present work, the GWO algorithm is relied upon for adjusting parameters of conventional PID control units to improve the performance of SM. Control the position of the rotor and determine the speed of the motor, with a target function to eliminate the error for transient cases such as ITAE, this type of technology depends on the location of the prey, how to determine the hunting behavior, generate a random number for the hunting group, determine the target function, and work on the estimation process and iterative operations to obtain the optimal location for the prey. The simulation results demonstrated the effectiveness and effectiveness of the proposed model. The speed of an electric motor can be controlled in many different ways, including by control systems and others by regulating voltage or frequency through the use of traditional units (PIC, PDC, PIDC) or expert (neural networks and fuzzy logic) as well as smart ones (PSO, Ant, and GWO). It is also possible to rely on adding electronic switching devices to control the input of the motors and the systems that include them [14]–[16].

2. RESEARCH METHOD

Electric motors in general are used in many applications, including industrial applications. In particular, the importance of using a stepper motor has emerged in many systems, as this type of motor can convert the electrical pulse into a step that moves the rotor according to an axis called the axis of movement of the rotor. The multiple movements required in a specific time and precise steps require a system capable of providing the required response according to an appropriate arrangement of those steps and in the correct arrangement of the signals. One of the problems of these systems is the failure of the engine to move with the required accuracy. Therefore, it is necessary to develop appropriate solutions and conduct tests to verify the possibility of improving performance and operation in various conditions. For system states and to obtain the required accuracy and similarity of work in real-time. It is also necessary to solve this problem and to achieve safe and accurate movement of the stepper motor according to a specific signal within times appropriate to the desired position. It was suggested to implement steps for experimental cases of a preliminary simulation model and obtain a design for a stepper motor system with highly efficient control units by conducting experiments on different formulas according to different degrees that suit the movement of the rotor of the stepper motor as reference values for the required input values, and following up and analyzing the response as it represents the movement of the rotor and at the appropriate times for each stepper motor case.

2.1. Mathematical and simulation model of stepper motors

In (1)-(7) represent a mathematical model of SM that demonstrates anchor chain, momentary driving for rotational motion, and reduced mass [3]. Where the motor voltage (Ud), engine resistance (Rs), motor current (id), inductance of the excitation winding (Ls), reduced resistance (zp), armature current (iq). Tension of the armature (Uq), angular velocity (ω), phase angle (Φ0), load moment (M), and moment of resistance (Mc). The radius of the wheels (R), the reduced mass of the road printer (mnp), the rolling friction coefficient of the wheels (f), the acceleration(a), and the mass of the carriage (m1). The mass of the wheels (m2), the moment of inertia of the wheel about its axis (I1), and the moment of the engine inertia (I∂β). This paper presents a simulation model that include the transfer function of SM with open loop, closed loop without a controller as well as PID controller, the total models can be shown in Figures 1-4. Figure 1 shows the Simulink model of the open loop system by using the toolbox as shown in Figure 1(a) and by using the M file as shown in Figure 1(b). Figure 2 shows the Simulink model of the closed-loop system without a controller using the toolbox as shown in Figure 2(a) and using the M file as shown in Figure 2(b). Figure 3 shows the Simulink model of the close loop system with PID controller by using the toolbox as shown in Figure 3(a) and by using the M file as shown in Figure 3(b). Figure 4 shows the Simulink model of the close loop system with GWO-PID controller by using the toolbox as shown in Figure 4(a) and by using the M file as shown in Figure 4(b).

$$U_d = R_S i_d + L_s \frac{di_d}{dt} - z_p \omega L_S i_q \quad (1)$$

$$U_q = R_S i_d + L \frac{di_d}{dt} - z_p \omega L_S i_q + z_p \Phi_q \quad (2)$$

$$I \frac{d\omega}{dt} = \mathrm{M} - \mathrm{M}_C \quad (3)$$

$$M = \frac{3}{2} z_p \Phi_o i_q \quad (4)$$

$$M_c = R m_{np} a + f(m_1 g + 2mg) \quad (5)$$

$$M_{np} = m_1 2m_2 + \frac{2(I_1 + I_{\partial\beta})}{R^2} \quad (6)$$

$$\text{The transfer function for stepper motor} = \frac{3.9}{0.004s^2 + 0.35s + 1} \quad (7)$$

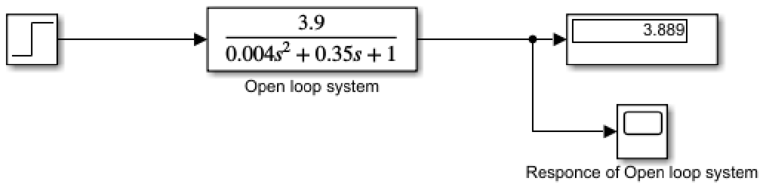

(a)

```
clc;clear all;close all;
ns=[3.9];
ds=[0.004 0.35 1];
G=tf(ns,ds);
step(G);
 title('Simulation and modeling for stepper motor');
xlabel('Time(sec)');
ylabel('Amplitude');
grid('on')
    legend('open loop')
```

(b)

Figure 1. Simulink model at open loop system in (a) by using toolbox and (b) by using M. file

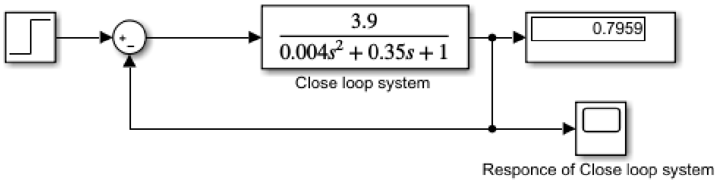

(a)

```
clc;clear all;close all;
ns=[3.9];
ds=[0.004 0.35 1];
G=tf(ns,ds);
Gf=feedback(G,1);
step(Gf);
 title('Simulation and modeling for stepper motor');
xlabel('Time(sec)');
ylabel('Amplitude');
grid('on')
```

(b)

Figure 2. Simulink model at close loop system without controller in (a) by using toolbox and (b) by using M. file

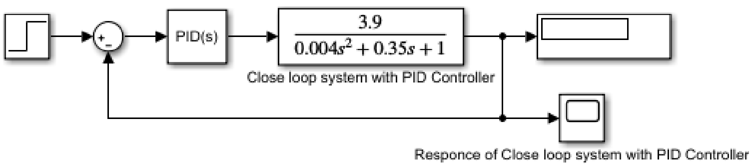

(a)

```
clc;clear all;close all;
ns=[3.9];
ds=[0.004 0.35 1];
G=tf(ns,ds);
Gf=feedback(G,1);
 Gc=pid(14.7682,28.7546,0.0739);
   Gcf=feedback(Gc*G,1);
    step(Gcf);
 title('Simulation and modeling for stepper motor');
xlabel('Time(sec)');
```

(b)

Figure 3. Simulink model at close loop system with PID Controller in (a) by using toolbox and (b) by using M. file

2.2. Implementation of stepper motors

Implementation of SM consists of two sections, first with PID Controller and second with advanced optimal by PID-GWO. The traditional PID controller is simple and used in many industrial processes, it can be represented in the transfer function which is indicated in (8) where Kp, Kd, and Ki are control parameters to be tuned for proportional, derivative, and integral terms, respectively [17], [18].

$$G_c = K_P + \frac{K_i}{s} + K_d S \tag{8}$$

The GWO algorithm includes four groups defined as a hierarchy of gray wolf populations that is as [19]–[22]:
- Alpha (α): Leaders in the alpha group are males and females and this group is responsible for making decisions (hunting, sleep, wake-up time);
- Beta (β): The beta group represents the second level in the hierarchy of gray wolves and is a subordinate wolf to the alpha wolf in decision-making or other activities;

- Delta (δ): the delta group is subject to the (alpha and beta) group, but it is the highest level of omega. This group belongs to (the elders, hunters, and those in charge of their care);
- Omega (ω): The wolves of the omega group are the lowest in rank play the role of scapegoats and are subject to the orders of the dominant wolves (alpha and beta).

Figure 5 shows a social hierarchy of GWO and the functions of the group's flowchart of GWO optimization can be shown in Figure 6.

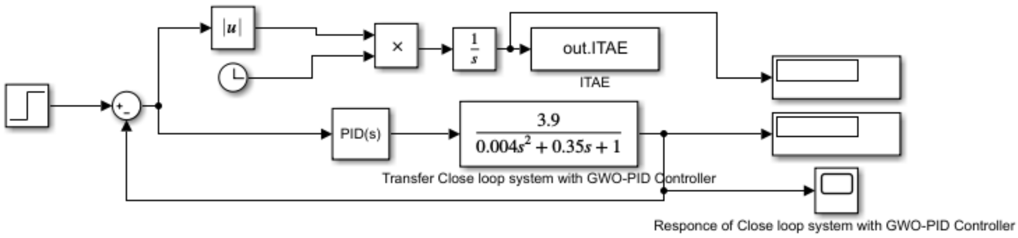

(a)

```
clc;clear all;close all;
ns=[3.9];
ds=[0.004 0.35 1];
G=tf(ns,ds);
Gf=feedback(G,1);
%GWO
iter=50;
pop=30;
a_gwo=10;
Var=3;
%Search Space
al=0;%Lower bound
au=50;%Upper bound
c_cf=0;
%initialization
for p=1:pop

    for n=1:Var
        x(p,n)=al+rand*(au-al);
    end
    %model parameter
    kp=x(p,1); ki=x(p,2); kd=x(p,3);
```

(b)

Figure 4. Simulink model at close loop system with GWO-PID controller in (a) by using toolbox and (b) by using M. file

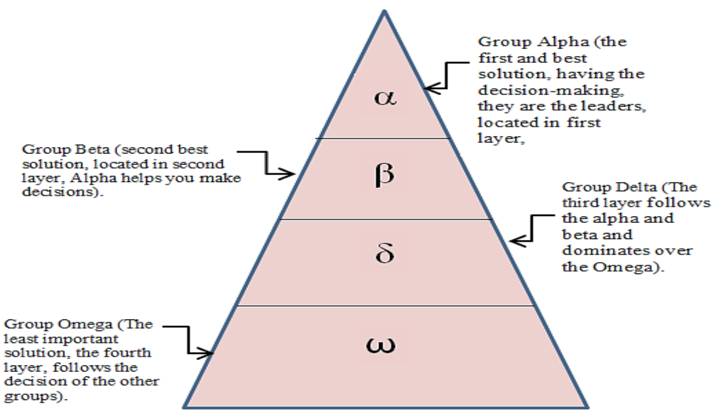

Figure 5. Social Hierarchy of GWO

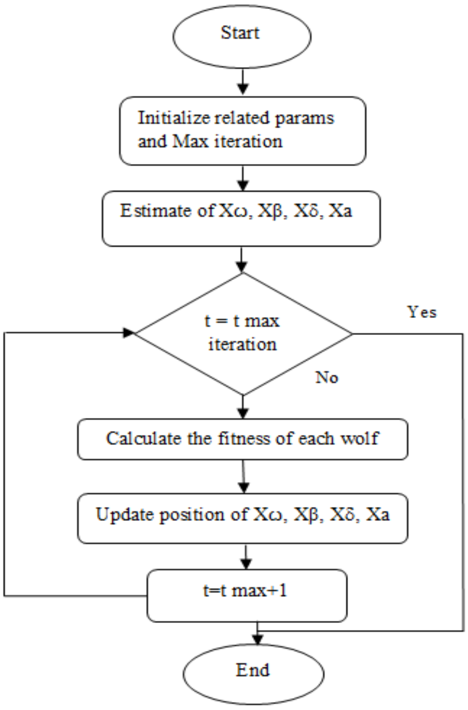

Figure 6. Flowchart of GWO

The objective function to obtain unknown controller parameters for PID controller to obtain optimization conditions and achieve stability for system response of SM, (fitness, objective function) taken is ITAE by the integral of time multiplied by absolute error and to improve the response of SM, ITAE is minimized. in (9) refers to the mathematical expression of ITAE. Where e(t) is the error signal that is the difference between reference and actual speed, Figure 7 shows the simulation model of ITAE [23]–[28].

$$ITAE = \int_0^{\infty} T|e(t)|dt \quad (9)$$

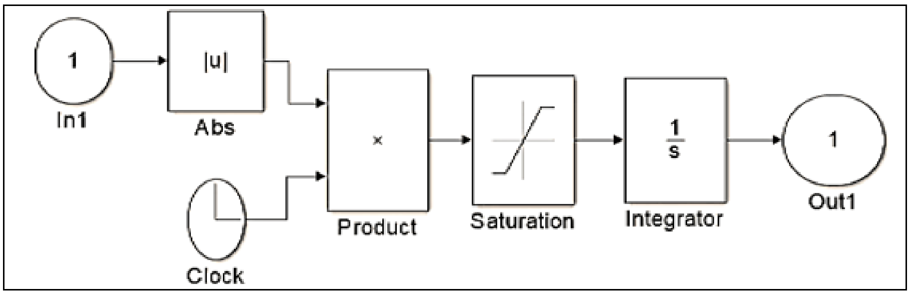

Figure 7. Simulation model of ITAE

3. RESULTS AND DISCUSSION

Under this heading, the current section contains two paragraphs: 3.1. Simulating and building the prototype, in which the prototype in Figures 1-4 is used to know the behavior of the system in different cases to obtain a suitable model that can be tested within the second paragraph of the same current section 3.2. Simulating and building the current proposed model after conducting the tests in the first paragraph, using the initial model, and after arriving at a suitable model through which the appropriate model can be implemented and operated for the cases proposed to be implemented, and its results will be shown in the following paragraphs.

3.1. Simulate and build the prototype

Using the simulation model in the first figure that shows the results of a stepper motor simulation, this research proposes SM simulation results using two cases: -The first open loop and closed loop without a controller while the second includes the use of controllers represented by PID and GWO-PID controllers. The first open loop, this part of the paper discusses the response of SM for each open and closed loop without using a controller which can be shown in Figures 8 and 9 respectively.

3.1.1. Simulation results without controller

The current paragraph includes a simulation of the initial model in Figure 1, which represents the engine in the operating state in the open-loop system. The results can be shown in Figure 8, the Simulink response of the open loop system by using the toolbox as shown in Figure 8(a) and by using M. File as shown in Figure 8(b). The second operating condition can be shown for the closed-circuit model as shown in Figure 9, the Simulink response of the closed-loop system by using the toolbox as shown in Figure 9(a) and by using the M file as shown in Figure 9(b), where the difference can be observed. The response times of the system according to the performance measure for each of the times of rise, stability, and upper and lower transgressions, as is the case with other cases that will be mentioned in the following paragraphs. From the simulation results a closed loop, it is clear that the values of each rise time, pre-shoot, overshoot, and undershoot are equal to 130.440 ms, 0.505%, 0.501%, and 1.077% respectively.

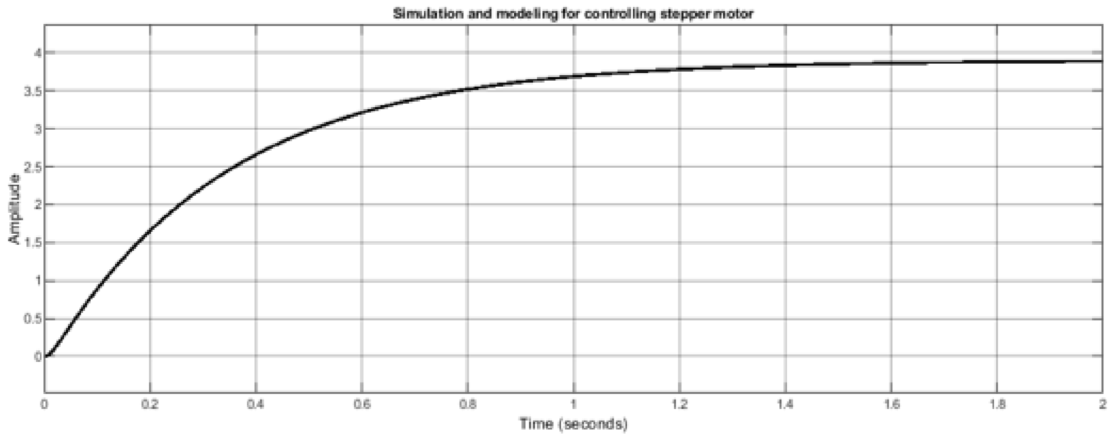

(a)

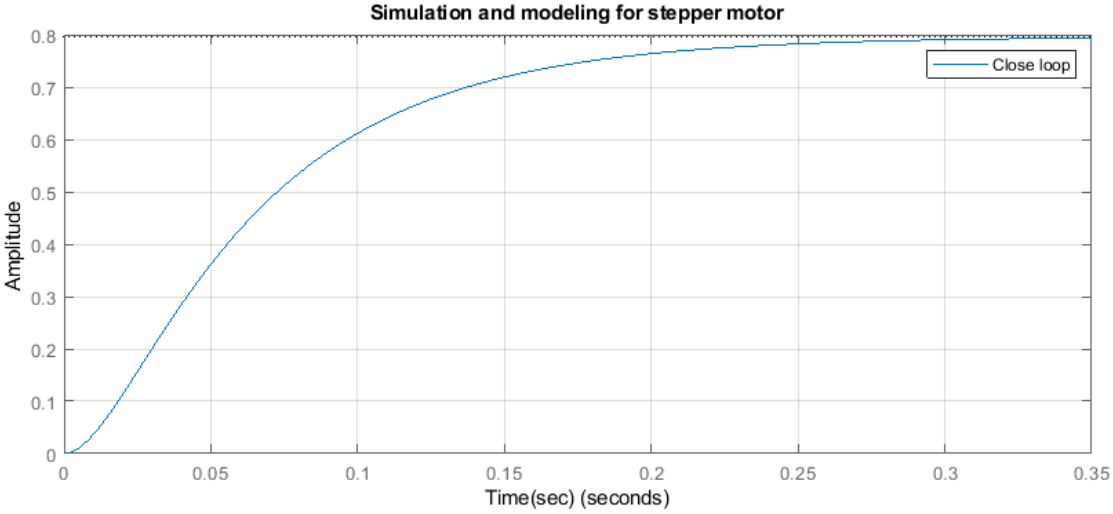

(b)

Figure 8. Simulink response at open loop system in (a) by using toolbox and (b) by using M. file

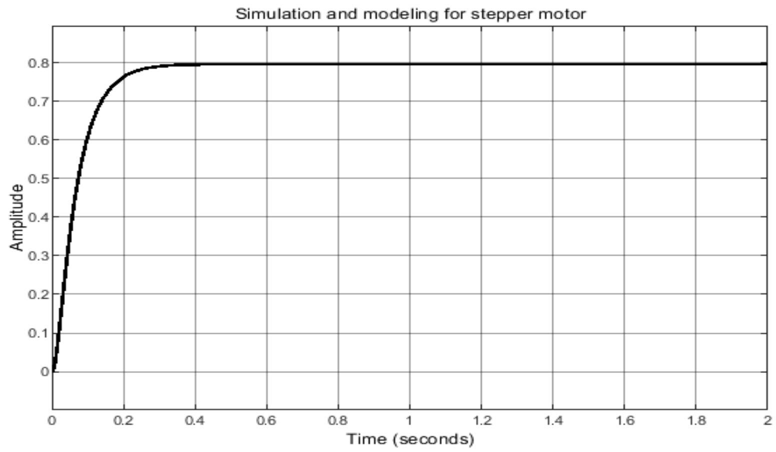

(a)

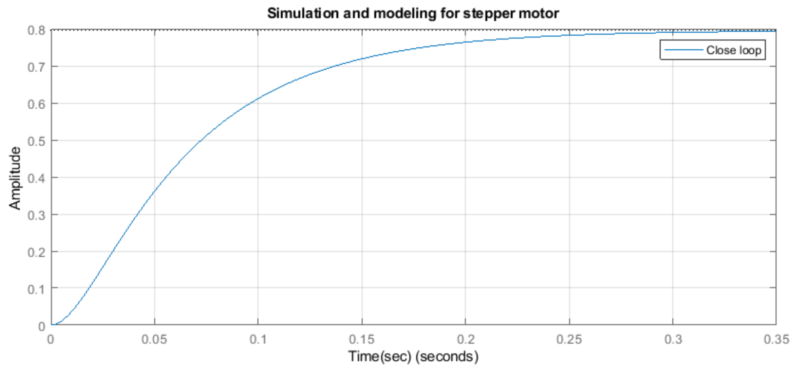

(b)

Figure 9. Simulink response at closed loop system in (a) by using toolbox and (b) by using M. file

3.1.2. Simulation results with controllers

This part deals with the discussion of the simulation results using the controllers which are PID and GWO-PID controllers. First when using the PID controller, the simulation results develop than previous cases and give a good response by reducing each overshoot, settling, and rise time. Values of overshoot=7.93%, settling time=0.0433, rise time=0.0134, values of controller parameters KP=14.7682, Kd=0.0739, and Ki=28.7546, Figure 10 shows the response of (SM) by using the PID controller. Figure 10 shows the Simulink response of the closed-loop system with PID controller using the toolbox as shown in Figure 10(a) and using the M file as shown in Figure 10(b).

3.1.3. With GWO-PID controller

To further improve the working of the SM, the GWO algorithm is used to estimate the best values of the controller constants (KP, Kd, and Ki) to achieve an optimization condition that can produce better results for the system. Figure 11 shows the step response of the SM using GWO-PID optimization. Figure 11 shows the Simulink response of the closed-loop system with GWO-PID controller using the toolbox as shown in Figure 11(a) and using the M file as shown in Figure 11(b).

From the observation of Figures 10 and 11 is clear that the results were developed by using GWO-PID over the previous cases by reducing values of overshoot to zero, rise time, and settling time to 0.00145, and 0.0027 respectively. The values of KP= 33.9940, Kd = 6.8326, and Ki=0 .429201, Figure 12 shows the objective function (ITAE).

From the simulation results, we note that the work has been developed through the use of the traditional PID controller by decreasing the overshoot values, and setting time and rise time. In the case of using the GWO-PID algorithm, the optimization condition was achieved by eliminating the overshoot and reaching zero and reducing values of settling time and rise time to values much lower than a case of the traditional PID controller Table 1 indicates to comparison of overshoot, settling time, rise time for system by using PID and GWO-PID controller, whereas Table 2 shows compare controlling parameters values.

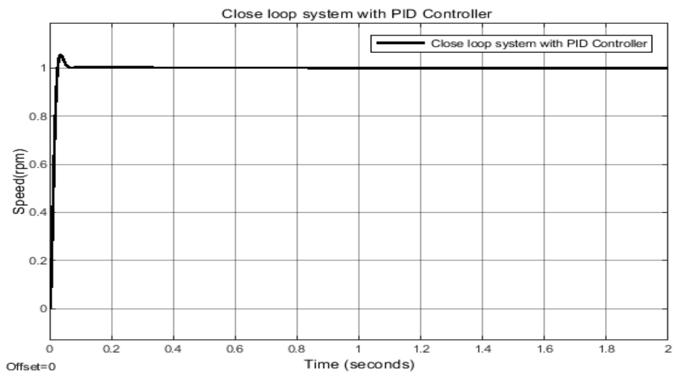

(a)

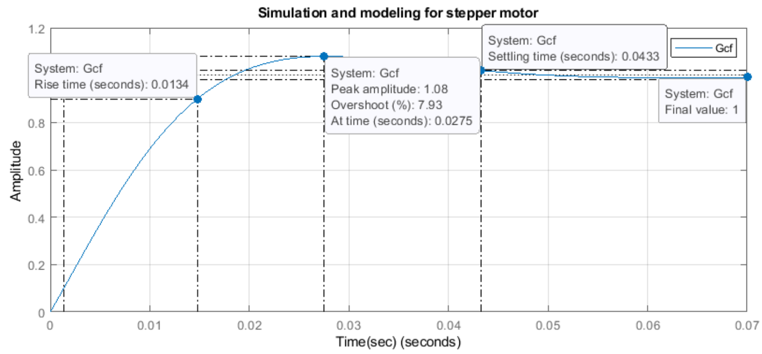

(b)

Figure 10. Simulink response at closed loop system with PID controller in (a) by using toolbox and (b) by using M. file

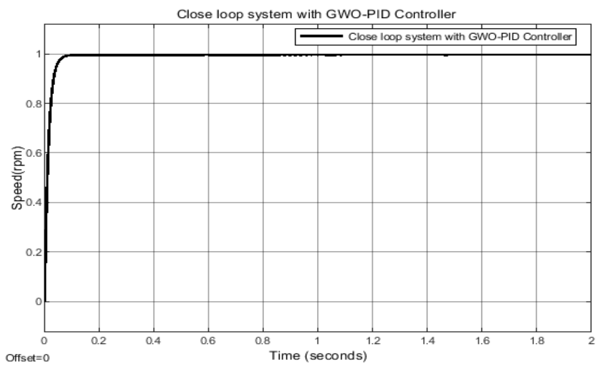

(a)

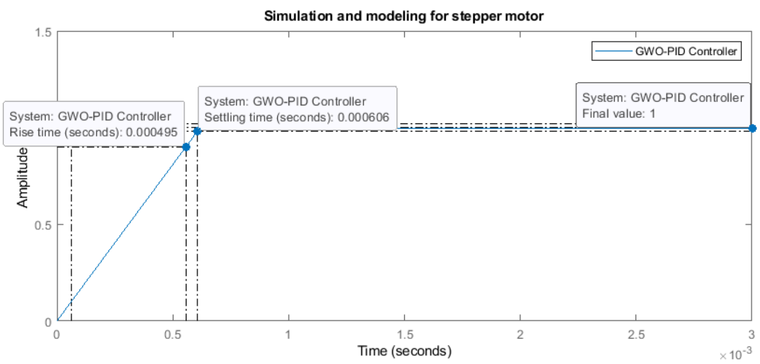

(b)

Figure 11. Simulink response at closed loop system with GWO-PID Controller in (a) by using toolbox and (b) by using M. file

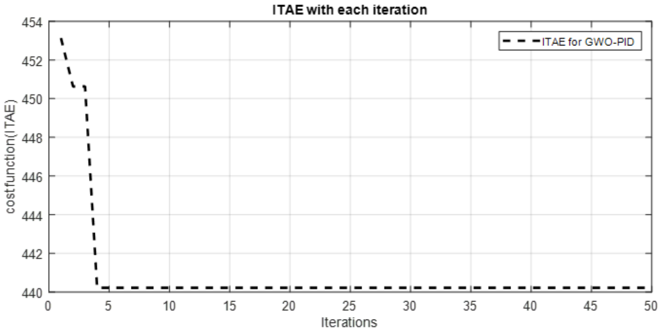

Figure 12. Convergence objective function (ITAE)

Table 1. Vales of overshoot, settling, and rise time

Controller types	Rise time (s)	Settling time (s)	Overshoot (%)
PID controller	0.0134	0.0433	7.93
GWO-PID controller	0.000495	0.000606	0

Table 2. Vales of PID parameters (kp, ki, and kd)

Controller types	kp	Ki	kd
PID controller	14.7682	0.0739	28.7546
GWO-PID controller	33.9940	6. 832	0.429201

3.2. Simulate and build the current proposed model

The electric motor has several steps, including rotating clockwise and counterclockwise in other steps to provide the required mechanical power. When the electric motor rotates in different steps in the same direction or the opposite direction, it takes different periods of time according to the appropriate mechanical force. The engine must be stopped before changing direction. Therefore, there are specific cases that must be included in the simulation model, for example, moving the engine clockwise, then stopping, then rotating it counterclockwise, then stopping, then moving clockwise, and so on. The proposed simulation cases are, firstly, the engine rotating at a constant speed and in a clockwise direction. Secondly, the engine rotates at a constant speed and in a counterclockwise direction. The proposed simulation cases are: Thirdly, the engine rotates at a variable speed and in a clockwise direction. Fourthly, the engine rotates at a variable speed and in a counterclockwise direction. Finally, the engine rotates in a clockwise direction, then the engine stops rotating, and the direction of movement changes, and so on.

A model of the electric motor can be built and represented to rotate according to the suggested steps, as follows: model number one, as in Figure 13, simulates the rotation of the motor clockwise to provide the required mechanical force. Figure 13 shows the simulated clockwise rotation of the motor to provide the required mechanical force in the simulation model as shown in Figure 13(a) and the simulation response as shown in Figure 13(b). It is also possible to represent and build another model of the rotation of the electric motor to rotate counterclockwise, in Figure 14, simulating rotating the motor counterclockwise to provide the required mechanical force. Figure 14 shows the model of the electric motor rotating counterclockwise in the simulation model as shown in Figure 14(a) and the simulation response as shown in Figure 14(b). The rotation of the electric motor in different steps in the same direction or in the opposite direction during different periods of time depending on the appropriate mechanical force can be built into a model as in Figure 15. Figure 15 shows the electric motor rotation model for clockwise and counterclockwise rotation in the simulation model as shown in Figure 15(a) and the simulation response as shown in Figure 15(b). The engine must be stopped before changing direction. Therefore, there are specific cases that must be included in the simulation model, for example, moving the engine clockwise, then stopping, then rotating counterclockwise, then stopping, then moving clockwise, and so on, as in the two models for both Figures 16 and 17. Figure 16 shows the model of the electric motor rotating clockwise, then stopping and moving clockwise in the simulation model as shown in Figure 16(a), and the simulation response as shown in Figure 16(b). Figure 17 shows the model of the electric motor rotating clockwise, stopping, and rotating counterclockwise in the simulation model as shown in Figure 17(a), and the simulation response as shown in Figure 17(b).

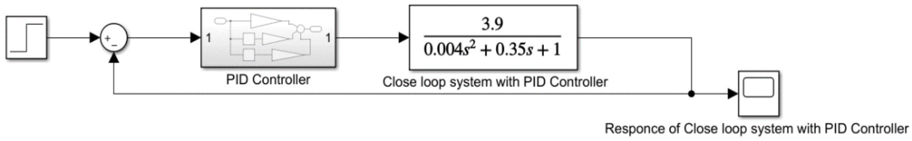

(a)

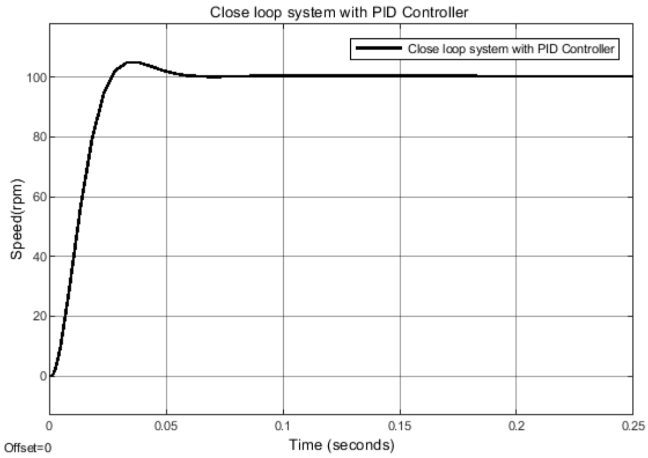

(b)

Figure 13. Simulates the rotation of the motor clockwise to provide the required mechanical force in (a) simulation model and (b) simulation response

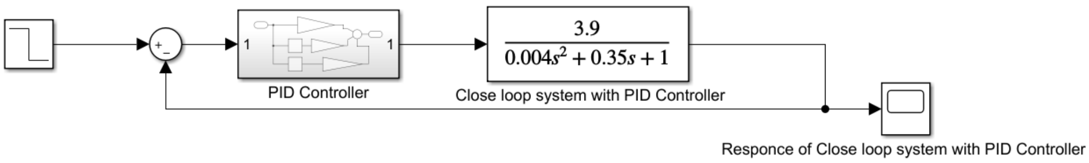

(a)

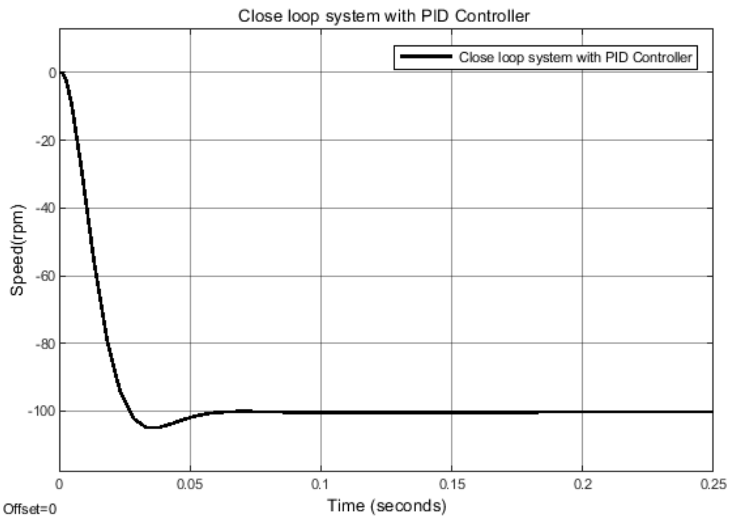

(b)

Figure 14. Model of the rotation of the electric motor to rotate counterclockwise in (a) simulation model and (b) simulation response

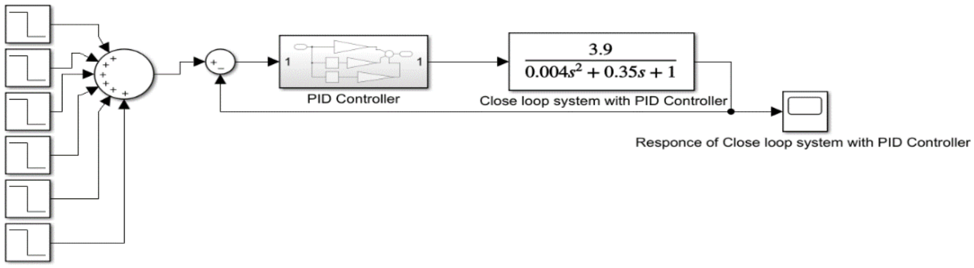

(a)

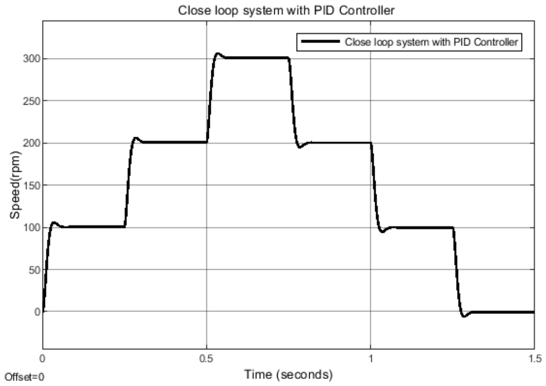

(b)

Figure 15. Model of the rotation of the electric motor to rotate clockwise and counterclockwise in (a) simulation model and (b) simulation response

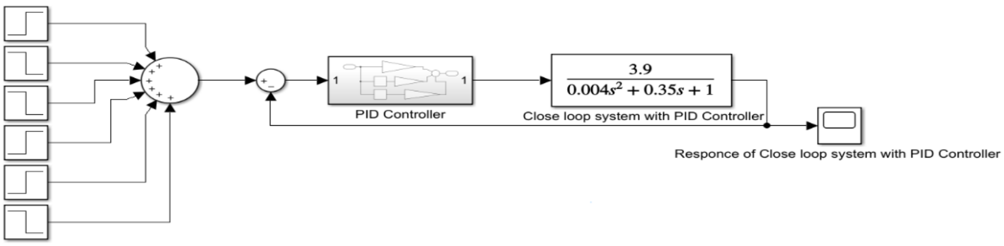

(a)

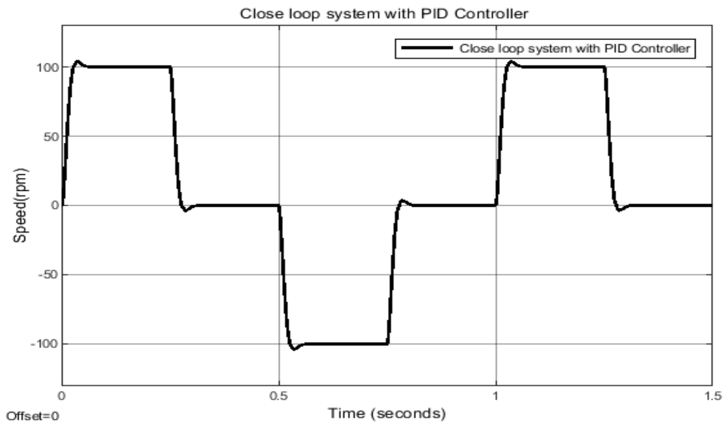

(b)

Figure 16. model of the rotation of the electric motor clockwise, then stopping then moving clockwise in (a) simulation model and (b) simulation response

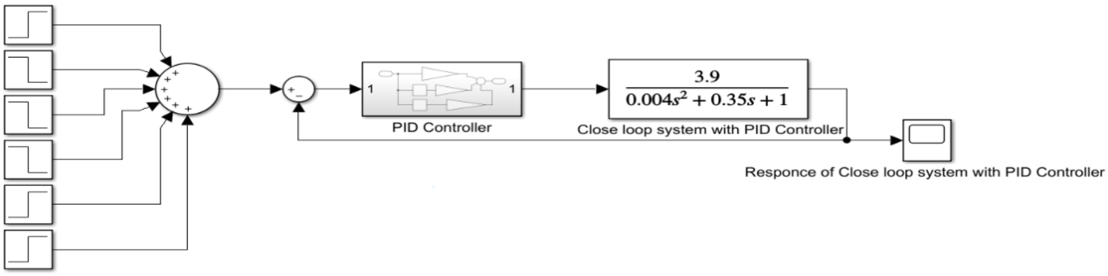

(a)

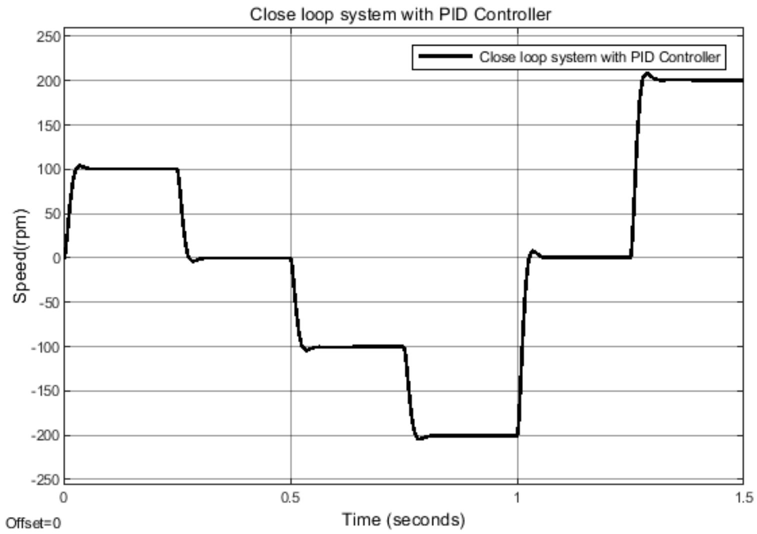

(b)

Figure 17. Model of the rotation of the electric motor clockwise, stopping and rotating counterclockwise in (a) simulation model and (b) simulation response

4. CONCLUSION

A computer simulation of the operating conditions of the stepping motor was conducted. Three working cases were proposed, such as the case of no control systems and another using the traditional system, as well as the use of optimal progress. Through the simulation results, a comparison was made between the proposed cases. The results showed the superiority of the gray wolf algorithm in adjusting the parameters of the traditional controller up to better performance than the case of using a traditional microcontroller. The comparison was made by adopting each of the accuracies, the speed of reaching the steady state, the average time of ascent, and the overrun and underpass for different work conditions that simulate real-time.

In the previous prototypes, tests were developed to arrive at a model design in which the proposed simulation cases could be implemented as a second stage of the researchers' work, obtaining the results of the proposed system, and analyzing the behavior of that system through its results. The proposed simulation cases are, firstly, the rotation of the engine at a constant speed and in a clockwise direction, whose model can be represented. Secondly, the rotation of the engine at a constant speed and in a counterclockwise direction, whose model can be represented. The proposed simulation cases are: Thirdly, the engine rotates at a variable speed and in a clockwise direction.

REFERENCES

[1] C. Wang and D. Cao, "New sensorless speed control of a hybrid stepper motor based on fuzzy sliding mode observer," *Energies*, vol. 13, no. 18, p. 4939, 2020, doi: 10.3390/en13184939.
[2] S. Suh and W. Kim, "Position control based on add-on-type iterative learning control with nonlinear controller for permanent-magnet stepper motors," *Applied Sciences*, vol. 11, no. 2, p. 587, 2021, doi: 10.3390/app11020587.
[3] R. T. Yemelyanov, A. S. Klimov, E. S. Turysheva, and V. V Servatinsky, "Travel printer with positional stepper motor control," in *IOP Conference Series: Materials Science and Engineering*, 2019, vol. 698, no. 7, p. 77002, doi: 10.1088/1757-899X/698/7/077002.

[4] M. Faus, F. Alonso, C. Fernández, and S. A. Useche, "Are traffic announcements really effective? A systematic review of evaluations of crash-prevention communication campaigns," *Safety*, vol. 7, no. 4, p. 66, 2021, doi: 10.3390/safety7040066.
[5] H. S. Dakheel, Z. B. Abdullah, N. S. Jasim, and S. W. Shneen, "Simulation model of ANN and PID controller for direct current servo motor by using Matlab/Simulink," *TELKOMNIKA (Telecommunication Computing Electronics and Control)*, vol. 20, no. 4, p. 922, Aug. 2022, doi: 10.12928/telkomnika.v20i4.23248.
[6] I. Hussain, D. C. Das, A. Latif, N. Sinha, S. M. S. Hussain, and T. S. Ustun, "Active power control of autonomous hybrid power system using two degree of freedom PID controller," *Energy Reports*, vol. 8, pp. 973–981, Nov. 2022, doi: 10.1016/j.egyr.2022.05.202.
[7] M. A. Ahmad, Z. Musa, M. H. Suid, and M. Z. M. Tumari, "Grey wolf optimizer for identification of liquid slosh behavior using continuous-time hammerstein model," *Bulletin of Electrical Engineering and Informatics*, vol. 9, no. 2, Apr. 2020, doi: 10.11591/eei.v9i2.2074.
[8] G. W. Abedulabbas and F. R. Yaseen, "Design a PI controller based on PSO and GWO for a brushless DC motor," *Journal Européen des Systèmes Automatisés*, vol. 55, no. 3, pp. 331–338, Jun. 2022, doi: 10.18280/jesa.550305.
[9] Y. Zhao, X. Yu, and J. Qi, "Speed control system of stepping motor based on BP neural network PID," in *2022 IEEE 10th Joint International Information Technology and Artificial Intelligence Conference (ITAIC)*, Jun. 2022, pp. 2280–2284. doi: 10.1109/ITAIC54216.2022.9836888.
[10] M. S. Mahmoud and A. H. A. Ramadhan, "Optimizing the parameters of sliding mode controllers for stepper motor through simulink response optimizer application," *International Journal of Robotics and Control Systems*, vol. 1, no. 2, pp. 209–225, Jul. 2021, doi: 10.31763/ijrcs.v1i2.345.
[11] M. Y. Silaa, O. Barambones, M. Derbeli, C. Napole, and A. Bencherif, "Fractional order PID design for a proton exchange membrane fuel cell system using an extended grey wolf optimizer," *Processes*, vol. 10, no. 3, p. 450, Feb. 2022, doi: 10.3390/pr10030450.
[12] G. A. Aziz, S. W. Shneen, F. N. Abdullah, and D. H. Shaker, "Advanced optimal GWO-PID controller for DC motor," *International Journal of Advances in Applied Sciences*, vol. 11, no. 3, p. 263, Sep. 2022, doi: 10.11591/ijaas.v11.i3.pp263-276.
[13] M. Magdi, M. El-Saadawi, E. A. Gouda, M. A. Elhosseini, and M. S. Essa, "Identification and speed control of DC motor using fractional order PID: microcontroller implementation," *EJECE, European Journal of Electrical and Computer Science*, vol. 4, no. 1, pp. 1–8, 2020, doi: 10.24018/ejece.2020.4.1.170.
[14] F. N. Abdullah, G. A. Aziz, and S. W. Shneen, "GWO-PID of two-phase hybrid stepping motor for robotic grinding force," *Journal of Fuzzy Systems and Control*, vol. 1, no. 3, pp. 71–79, Nov. 2023, doi: 10.59247/jfsc.v1i3.91.
[15] S. W. Shneen, "Advanced optimal for three phase rectifier in power-electronic systems," *Indonesian Journal of Electrical Engineering and Computer Science*, vol. 13, no. 5, pp. 821–830, 2018.
[16] T. Prakash, V. P. Singh, and N. Patnana, "Gray wolf optimization-based controller design for the two-tank system," in *Applications of Artificial Intelligence Techniques in Engineering*, 2019, pp. 501–507, doi: 10.1007/978-981-13-1819-1_47.
[17] B. Nail and B. Bekhiti, "Optimal PID controllers design for discharge pressure-temperature control of centrifugal gas compressor system using grey wolf optimizer," *Recueil de mécanique*, vol. 6, no. 2, pp. 629–636, 2022.
[18] N. Priyadarshi, S. Padmanaban, M. S. Bhaskar, F. Azam, B. Khan, and M. G. Hussien, "A novel hybrid grey wolf optimized fuzzy logic control based photovoltaic water pumping system," *IET Renewable Power Generation*, Nov. 2022, doi: 10.1049/rpg2.12638.
[19] I. J. Mwakitalima, M. Rizwan, and N. Kumar, "Potential of a nonperennial tributary integrated with solar energy for rural electrification: a case study of Ikukwa Village in Tanzania," *Mathematical Problems in Engineering*, vol. 2022, pp. 1–37, May 2022, doi: 10.1155/2022/1172050.
[20] S. Mirjalili, S. M. Mirjalili, and A. Lewis, "Grey wolf optimizer," *Advances in Engineering Software*, vol. 69, pp. 46–61, Mar. 2014, doi: 10.1016/j.advengsoft.2013.12.007.
[21] I. Khanam and G. Parmar, "Application of SFS algorithm in control of DC motor and comparative analysis," in *2017 4th IEEE Uttar Pradesh Section International Conference on Electrical, Computer and Electronics (UPCON)*, Oct. 2017, pp. 256–261. doi: 10.1109/UPCON.2017.8251057.
[22] A. Ahmed, R. Gupta, and G. Parmar, "GWO/PID approach for optimal control of DC motor," in *2018 5th International Conference on Signal Processing and Integrated Networks (SPIN)*, Feb. 2018, pp. 181–186. doi: 10.1109/SPIN.2018.8474105.
[23] H. S. Dakheel, Z. B. Abdullah, and S. W. Shneen, "Advanced optimal GA-PID controller for BLDC motor," *Bulletin of Electrical Engineering and Informatics*, vol. 12, no. 4, pp. 2077–2086, Aug. 2023, doi: 10.11591/eei.v12i4.4649.
[24] H. S. Dakheel, Z. B. Abdulla, H. J. Jawad, and A. J. Mohammed, "Comparative analysis of PID and neural network controllers for improving starting torque of wound rotor induction motor," *TELKOMNIKA (Telecommunication Computing Electronics and Control)*, vol. 18, no. 6, p. 3142, Dec. 2020, doi: 10.12928/telkomnika.v18i6.14571.
[25] S. W. Shneen, F. N. Abdullah, and D. H. Shaker, "Simulation model of single phase PWM inverter by using MATLAB/Simulink," *International Journal of Power Electronics and Drive Systems (IJPEDS)*, vol. 12, no. 1, p. 212, Mar. 2021, doi: 10.11591/ijpeds.v12.i1.pp212-216.
[26] Q. Ali and M. Ezzaldean, "Direct current deadbeat predictive controller for BLDC motor using single DC-link current sensor," *Engineering and Technology Journal*, vol. 38, no. 8, pp. 1187–1199, Aug. 2020, doi: 10.30684/etj.v38i8A.471.
[27] R. Raheem, M. Y., and S. Kadhim, "Simulation design of blood-pump intelligent controller based on PID-like fuzzy logic technique," *Engineering and Technology Journal*, vol. 38, no. 8, pp. 1200–1213, Aug. 2020, doi: 10.30684/etj.v38i8A.534.
[28] A. Jassim, A. Issa, and Q. Jawad, "A hybrid neural-fuzzy network based fault detection and isolation system for DC motor of robot manipulator," *Engineering and Technology Journal*, vol. 37, no. 8A, pp. 326–331, Aug. 2019, doi: 10.30684/etj.37.8A.3.

BIOGRAPHIES OF AUTHORS

Salam Waley Shneen educational background: July 2016 Ph.D., degree in electrical engineering-power electronic, School of Electrical and Electronic Engineering, Huazhong University of Science and Technology (HUST). Nov 2005 M.Sc., degree in engineering educational technology-electrical engineering, Technical Education Department, University of Technology, Iraq-Baghdad. July 1998 B.Sc., a degree in electrical engineering and education, Technical Education Department, University of Technology, Iraq-Baghdad. Oct 1994 diploma in electrical technology, Technical Instructors Training Institute, Iraq Baghdad. 1992 High School Bakaloria Degree Preparatory Technical School (Electrical Section), Al Mashtal Technical Secondary School Iraq-Baghdad. Work Experience 1998-2005 Engineer in: Electronic Lab., Digital Electronic Lab., Communication Lap., Fundamental of Electric Engineering Lab. Cad Lab. In Technical Education Department, University of Technology, Iraq-Baghdad. 2005-2016 Assistant Lecturer in: Electronic Lab. Lecturer Advanced Electronic, Lecturer Fundamental of Electric Engineering, Technical Education Department, Electromechanical Department University of Technology, Iraq-Baghdad. 2016-2017 Lecturer in Electronic Lab. Fundamental of Electric Engineering Lab., Lecturer Electronic Circuits, Lecturer Fundamental of Electric Engineering with Electrical and Electronic Circuits Electromechanical Department University of Technology, Iraq-Baghdad. 2017-10Apr.2022 Lecturer in: Energy and Renewable Energies Technology Center, University of Technology, Iraq-Baghdad. 10 Apr.2022- today Lecturer in Nanotechnology and advanced material research Center, University of Technology, Iraq-Baghdad. He can be contacted at emails: salam_waley73@yahoo.com and 50054@uotechnology.edu.iq.

Hashmia S. Dakheel is a lecturer at the Department of Electromechanical Engineering, University of Technology, Iraq, she obtained a master degree in electrical engineering from the University of Technology in 2000, and a bachelor's degree in electrical engineering from the University of Technology, Iraq in 1994, her research areas are electrical engineering and electrical machines. She can be contacted at email: Hashmia.S.Dakheel@uotechnology.edu.iq.

Zainab B. Abdullah is a lecturer at the Department of Electromechanical Engineering, University of Technology, Iraq She obtained a bachelor's degree in electrical engineering from the University of Technology-Iraq in 1994, and a master degree in engineering educational technology, and electrical engineering from the University of Technology-Iraq, in 2001. Her research areas are electrical engineering and electric machines. She can be contacted at email: Zainab.B.Abdullah@uotechnology.edu.iq.